Effects of Cobalt on the Crystalline Structures of the Ni-Mn-In Giant Magnetocaloric Heusler Alloys

Amila Madiligama, P. Ari-Gur, V. Shavrov, V. Koledov, Y. Ren, S. Calder and A. Kayani

Abstract The giant inverse magnetocaloric effect driven by a merged magneto-structural transformations in Ni-Mn-In-Co Heusler alloys, makes them highly promising as solid state refrigerants near room temperature. Knowledge of the crystallographic behavior of these alloys at a broad temperature range is critical to the understanding of the giant magnetocaloric effect. In this study, three Ni-Mn-In-Co alloys were investigated by neutron and synchrotron diffraction techniques. The chemical compositions of the alloys, determined by the Rutherford Backscattering Spectrometry (RBS) technique, were $Ni_{41}Mn_{39}In_{12}Co_{8,}$ $Ni_{48}Mn_{34}In_{12}Co_6$ and $Ni_{52}Mn_{25}In_{16}Co_7$. The austenitic (A) phase of all three alloys was cubic $L2_1$ ($Fm\bar{3}m$). Martensitic (M) phase of the $Ni_{41}Mn_{39}In_{12}Co_8$ alloy was a mix of 8M and 6M modulated monoclinic structures, while the other two alloys had a M composed of a mix of 7M and 5M modulated monoclinic structures. All modulated structures belong to the P 1 2/m 1 space group. Site occupancy refinements of the A phases of all three alloys, revealed that almost all the Co atoms ($\sim$97%) occupy the regular Ni (8c) sites. In the studied temperature range (50–250 K) of the M phase of the $Ni_{41}Mn_{39}In_{12}Co_8$ alloy has very low magnetization. Also, no antiferromagnetic ordring was observed in the neutron diffraction refinement of the M phase. Therefore by eliminating the possibilities of ferromagnetism and antiferromagnetism, it is concluded that the M phase of the $Ni_{41}Mn_{39}In_{12}Co_8$ alloy is spin glass.

A. Madiligama (✉) · P. Ari-Gur · A. Kayani
Western Michigan University, Kalamazoo, MI 49008, USA
e-mail: amila.bandara@wmich.edu

V. Shavrov · V. Koledov
Kotelnikov Institute of Radio-Engineering and Electronics of RSA, Moscow, Russia

Y. Ren
Advanced Photon Source, Argonne National Laboratory, 60439 Argonne, IL, USA

S. Calder
Quantum Condensed Matter Division, Oak Ridge National Lab, Oak Ridge, TN, USA

A.Y. Oral et al. (eds.), *2nd International Congress on Energy Efficiency and Energy Related Materials (ENEFM2014)*, Springer Proceedings in Energy,
DOI 10.1007/978-3-319-16901-9_62

1 Introduction

Magnetic cooling technology based on the Magnetocaloric Effect (MCE), has been known for more than a century. Even so, a proof of concept of a feasible magnetic cooling system, working near room temperature, was first introduced in 1997 [1]. The growth this technology depends on suitable magnetocaloric materials; those are readily available, durable, economically feasible, and work under moderate magnetic fields. A large magnetocaloric effect is usually exhibited by magnetic materials that undergo first-order magneto-structural phase transformations [2].

Among other competitors, which exhibit first-order magnetic phase transitions, Ni-Mn-X (X = In, Sb, Sn) Heusler alloys gain considerable attention because of their first-order, metamagnetic phase transformations, which occurs near room temperature [3]. For instance, large MCE was reported in a number of Ni-Mn-X alloys such as, Ni-Mn-In [4], Ni-Mn-Sn [5], and Ni-Mn-Sb [6]. At a certain temperature range, under sufficient magnetic field, Ni-Mn-X alloys transform from the low symmetry, martensitic (M) phase to higher symmetry austenitic (A) phase. The large cooling effect observed here is mostly due to the structural transition from M to A phase. Nevertheless, the contribution from spin alignment is also important as the driving force of the magnetostructural transformations [3]. For a wide range of compositions, the A phase of these alloys is cubic $L2_1$ [3, 7–9]. However, depending on the compositions, the M structure could be a single phase or a mix of two phases. Non-modulated $L1_0$ [9], 5M modulated orthorhombic [8, 10], 5M [3, 8], 6M [9] and 7M modulated monoclinic [8], and a mix of 5M and 7M modulated martensite [7] are some of the structures reported for the M phase. The substitution of a small percentage of Co for Ni in Ni-Mn-X alloys significantly increases the MCE [3]. Additionally, Co makes it possible to tune the M transformation temperature [11]. To develop these Ni-Mn-In-Co alloys as better magnetocaloric materials, a thorough understanding of the effects of Co substitution on crystalline structure and magnetic ordering is essential. Thus, the primary objectives of the present study were to determine the structures, chemical order, and magnetic ordering of the M phase as a result of Co substitution.

2 Experimental Techniques and Sample Preparation

Polycrystalline samples were prepared by the arc-melting method. Sample 03 ($Ni_{41}Mn_{39}In_{12}Co_8$) was used in the as-cast state. The others were heat treated by annealing for 50 h at 1020 K. The chemical compositions of the alloys were determined by the RBS technique using 15 MeV O^{+4} ion beam. The RBS experiment was carried out at the 6 MeV tandems Van de Graaff accelerator at Western Michigan University. The RBS data were analyzed by SIMNRA [12]. Neutron diffraction measurements of the $Ni_{41}Mn_{39}In_{12}Co_8$ alloy were carried out in the high-resolution constant wavelength (0.15374 nm) neutron powder diffractometer

HB2A at Oak Ridge National Laboratory [13]. Data were collected at different temperatures in the range, 50–600 K. In situ synchrotron diffraction measurements of the $Ni_{48}Mn_{34}In_{12}Co_6$ and $Ni_{52}Mn_{25}In_{16}Co_7$ alloys were carried out at beamline 11-ID-C of the Advanced Photon Source at Argonne National Laboratory [14], using a wavelength of 0.0108040 nm. Diffraction data were collected at different temperatures and under different magnetic fields. Rietveld refinements of both the neutron and synchrotron diffraction data were carried out using GSAS [15] and GSAS EXPGUI [16].

3 Results and Discussion

In the RBS experiment, the projectile ion type, energy of the ion beam and scattering angle were selected to maximize the energy resolution between scattered ions from the Ni and Co atoms, which have similar atomic masses. The chemical compositions of the alloys determined by the RBS technique are summarized in Table 1.

A critical aspect of this experiment was the accurate determination of site occupancies of the Co atoms. Even small changes in the magnetic interactions of Co with other atoms with different magnetic moments (Ni and Mn) greatly affects the magnetic behavior. Three different crystallographic sites, 4a, 4b, and 8c, (regular sites of Mn, In and Ni respectively), can potentially be occupied by the Co atoms. To determine the chemical order, site occupancy refinements of the neutron diffraction data of the $Ni_{41}Mn_{39}In_{12}Co_8$ alloy, collected at 3 different temperatures (600, 450 and 400 K) in the A phase, were carried out. The site occupancy refinements of the A phase of the other two alloys were carried out using their synchrotron diffraction data collected at 300 K. In the refinements, all the possible ways of occupying a crystallographic site by each atom were considered; the results are summarized in Table 2. The site occupancy results revealed that $\sim$97% of the substituted Co atoms occupy the regular Ni sites and the rest in the Mn sites. This observation is in good agreement with the formation energy calculations of the A phase carried out by J. Bai et al., that studied the site preference of Co in Ni-Mn-Ga alloy [17]. In all 3 alloys, the regular In sites are occupied by both Mn and In atoms, with approximately 50% of each Mn and In. Mn atoms occupy all 3 sites. However,

Table 1 Summary of the RBS analysis of the 3 alloys, calculated elemental compositions

Alloy	Incident/scattering angle (°)	Ni	Mn	In	Co
$Ni_{52}Mn_{25}In_{16}Co_7$	0/150	52.19 ± 0.40	24.89 ± 0.62	16.02 ± 0.23	6.96 ± 0.98
$Ni_{41}Mn_{39}In_{12}Co_8$	0/150	40.68 ± 0.30	39.22 ± 0.23	11.60 ± 0.12	8.50 ± 0.65
$Ni_{48}Mn_{34}In_{12}Co_6$	0/150	47.98 ± 0.33	33.74 ± 0.30	12.38 ± 0.27	5.96 ± 0.90

Table 2 Summary of the site occupancy refinements of the alloys ($Ni_{52}Mn_{25}In_{16}Co_7$–01, $Ni_{48}Mn_{34}In_{12}Co_6$–02, and $Ni_{41}Mn_{39}In_{12}Co$–03) in the A phase at different temperatures

Alloy	T (K)	Cyst. Site	Occupation of each site (%)				Elemental composition (%)			
			Ni	Co	Mn	In	Ni	Co	Mn	In
01	300	4a	37.68	0	62.32	0	52.40	7.42	24.10	15.51
		4b	0	0	33.95	62.05				
		8c	85.96	14.80	0	0				
02	300	4a	15.40	0	84.60	0	48.05	5.81	34.19	11.95
		4b	0	0	52.17	47.83				
		8c	88.40	11.6	0	0				
03	400	4a	3.31	1.32	95.6	0	39.90	8.71	39.20	11.70
		4b	0.81	0	53.3	46.8				
		8c	79.3	16.8	4.03	0				
	450	4a	5.11	0	94.9	0	40.80	8.06	39.60	12.00
		4b	0	0	51.3	48				
		8c	79	16.1	6.04	0				
	600	4a	2.58	0	97.4	0	40.30	8.39	39.50	11.80
		4b	0	0	52.1	47.2				
		8c	79.2	16.8	4.16	0				

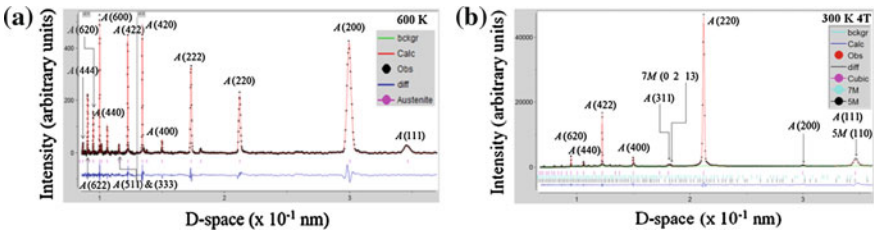

Fig. 1 Refinements of the A phase of two alloys. **a** Neutron diffraction of the $Ni_{41}Mn_{39}In_2Co_8$ alloy collected at 600 K and **b** synchrotron diffraction of $Ni_{52}Mn_{25}In_{16}Co_7$ alloy collected at 300 K under 4 T applied magnetic field

most of the Mn atoms are concentrated in the regular Mn sites. Compositions calculated by site occupancy refinements show a good agreement with the values obtained by RBS analysis. The final compositions of the alloys were determined to be $Ni_{41}Mn_{39}In_{12}Co_8$, $Ni_{48}Mn_{34}In_{12}Co_6$ and $Ni_{52}Mn_{25}In_{16}Co_7$ (Fig. 1).

The crystalline structures of $Ni_{41}Mn_{39}In_{12}Co_8$ alloy at various temperatures in the range from 50 to 600 K was found by refinements of the neutron diffraction data; while the structures of the other two alloys were found by refinements of their synchrotron diffraction data. Above the M transformation temperature, the structure of all 3 alloys was found to be cubic $L2_1$ ($Fm\bar{3}m$) with similar lattice parameters. In the refinements of modulated M structures, the following steps were taken to reduce the number of refinement parameters [18–20]: (1) the lattice modulation occurs

Table 3 Agreement factors [16] of the refinements and lattice parameters of different phases

Alloy	T (K)	Structure	a (nm)	b (nm)	c (nm)	β (°)	R_{wp}	R_p	χ^2
01	300	A	0.599	0.599	0.599	90	6.7	4.2	3.3
	205	5 M/7 M	0.451/ 0.427	0.580/ 0.548	2.254/ 2.863	89.12/ 91.05	2.9	1.8	1.1
02	300	A	0.599	0.599	0.599	90	5.7	4.2	4.6
	230	5 M/7 M	0.450/ 0.427	0.577/ 0.551	2.252/ 2.859	89.26/ 91.28	3.0	1.9	1.2
03	600	A	0.601	0.6007	0.601	90	4.9	3.6	3.1
	250	6 M/8 M	0.440/ 0.443	0.554/ 0.557	2.582/ 2.3.288	93.65/ 91.05	1.9	1.4	1.2

along the [001] direction of the monoclinic unit cell (the [110] direction of the A phase), (2) both x and y coordinates of all atoms in the M phase were allowed to refine, while the z coordinate was kept constant, (3) because the modulation involves the periodic transversal displacements of (001) atomic layers, the amplitude of modulation of every atom in that plane was taken to be the same value. Crystalline structures of the M phase of $Ni_{48}Mn_{34}In_{12}Co_6$ and $Ni_{53}Mn_{25}In_{15}Co_7$ alloys were found to be a mixture of two monoclinic structures with 5M and 7M modulations (P 1 2/m 1). Even though they have significantly different compositions, their crystalline structures and lattice parameters are very similar. The M crystalline structure of the $Ni_{41}Mn_{39}In_{12}Co_8$ alloy was different from the rest. It was a mix of 6M and 8M modulated monoclinic structures (P 1 2/m 1). All modulated martensite have similar **a** and **b** lattice parameters. However, the **c-axis** and the modulation vary. Lattice parameters of all the structures in both phases and the agreement factors [16] of the respective refinement cycle are summarized in Table 3.

Below 250 K, $Ni_{41}Mn_{39}In_{12}Co_8$ alloy is a mixture of M phases. According to the thermomagnetic measurements, the magnetization of the M phase is very low compared to the A phase [21]. Therefore, the possible magnetic structures for the M phase of this alloy are either antiferromagnetic or disordered spin glass. Three of the constituent atoms of this alloy, (Ni, Mn, and Co), have net magnetic moments that interact with the neutrons. If there is any antiferromagnetic ordering present in the M phase, there should be extra diffraction peaks that belong to the antiferromagnetic ordering because the magnetic structure is enlarged compared to the M crystalline structure. Refinement of the neutron diffraction data (Fig. 2a) collected below the M transformation temperature (250 K), shows a very good agreement with the experimental diffraction pattern even at the small d spacing values (Fig. 2b). No additional diffraction peaks which could belong to the antiferromagnetic ordering were observed. Therefore, by elimination of other possibilities, it can be concluded that the M phase of the $Ni_{41}Mn_{39}In_{12}Co_8$ alloy is spin glass. In order to confirm the spin glass nature of the M phase of this alloy, diffuse neutron diffraction studies are planned. In other circumstances, AC-SQUID would have been another option; it is impossible, however, to carry these measurements due to

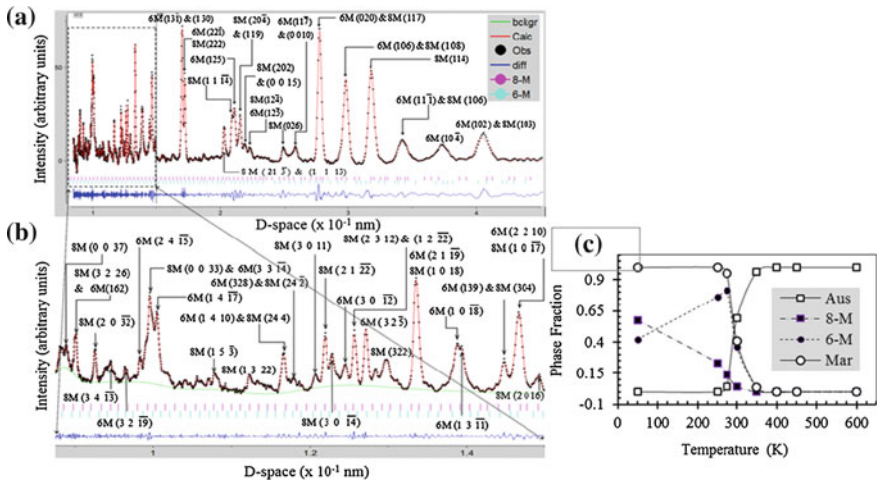

Fig. 2 **a** Rietveld refinements of neutron diffraction data of the $Ni_{41}Mn_{39}In_{12}Co_8$ alloy collected at 250 K (alloy is a mix of two martensitic phases: 6M & 8M martensite. **b** An enlarged portion of the diffraction pattern up to d spacing is 0.15 nm. **c** Variation of the phase fractions of the A and M phases from 50 to 600 K

the high transformation temperature. All the Co atoms reside in the regular Ni sites. Mn atoms are present in all 3 crystallographic sites. Ni atoms occupy both regular Ni and regular Mn sites. Therefore, the atoms which contribute to the magnetization, occupy randomly all crystallographic sites in the A phase. During the diffusionless M transformation, the magnetic disorder increases with the modulation of the M structures. This highly disordered distribution of magnetic moments in the M phase could lead to spin glass disorder.

Phase Fractions of the $Ni_{41}Mn_{39}In_{12}Co_8$ alloy at each temperature in the range from 50 to 600 K were calculated by the refinement. The studied temperature range can be classified into 3 regions (Fig. 2c). In the first region (600–350 K) the alloy is a single-phase austenite. In the second region (350–270 K), all 3 phases, austenite, 6M and 8M martensite co-exist. Nevertheless, the weight fraction of the 8M modulated phase is less than 5%. In the final region (275–50 K) two M phases, 6M and 8M modulations coexist. In this region, the weight fraction of the 6M martesite, the dominant phase below transformation temperature, decreases with decreasing temperature, which is compensated by the increase in the fraction of the 8M martensite and it dominates at 50 K. This behaviour of M phases results from the entropy of the structures; the highly ordered 8M modulated phase has lower entropy than the 6M modulated phase. Therefore, 8M modulated structures are energetically favorable at lower temperatures.

4 Conclusions

The compositions of the alloys determined by the RBS technique were found to be $Ni_{41}Mn_{39}In_{12}Co_{8,}$ $Ni_{48}Mn_{34}In_{12}Co_6$ and $Ni_{52}Mn_{25}In_{16}Co_7$. These values show a good agreement with the compositions calculated by the site occupancy refinements. For all 3 alloys, the A structure was cubic $L2_1$ ($Fm\bar{3}m$). However, the M phase of the $Ni_{41}Mn_{39}In_{12}Co_8$ alloy was a mix of 6M and 8M modulated structures, while that of the other two alloys was a mix of 5M and 7M modulated monoclinic structures. No antiferromagnetic ordering was observed in the M phase of the $Ni_{41}Mn_{39}In_{12}Co_8$ alloy. According to the thermomagnetic measurements, magnetization of the M phase is very low compared to the A phase. Therefore, it could be concluded that the spin glass magnetic disorder in the M phase of the $Ni_{41}Mn_{39}In_{12}Co_8$ alloy. The modulations of the M structures and highly disordered distribution of the magnetic moments in the M phase could lead to spin glass. In order to confirm the magnetic ordering in the M phase, diffuse scattering studies of the $Ni_{41}Mn_{39}In_{12}Co_8$ alloy are planned.

Acknowledgments This work was supported by Award No. RUP1-7028-MO-11 of the US Civilian Research & Development Foundation (CRDF Global) and by the National Science Foundation under Cooperative Agreement No. OISE-9531011. The authors also wish to acknowledge the US National Science Foundation award number NSF-0831951. Research at Oak Ridge National Laboratory was sponsored by the Scientific User Facilities Division, Office of Basic Energy Sciences and the US Department of Energy. APS use was supported by the US Department of Energy, Office of Science, under Contract No. DE-AC02-06CH11357. Last but not least, the authors wish to acknowledge Amila Dissanayake of the Department of Physics, Western Michigan University for his help in RBS experiments.

References

1. K.A. Gschneidner Jr., V.K. Pecharsky, A.O. Tsokol, Rep. Prog. Phys. **68**, 1479 (2005)
2. V.K. Pecharsky, J.K.A. Gschneidner Jr., Phys. Rev. Lett. **78**, 4494 (1997)
3. J. Liu, T. Gottschall, K.P. Skokov, J.D. Moore, O. Gutfleisch, Nat. Mater. **11**(7), 620 (2012)
4. Z.D. Han, D.H. Wang, C.L. Zhang, S.L. Tang, B.X. Gu, Y.W. Du, Appl. Phys. Lett. **89**, 182507 (2006)
5. T. Krenke, E. Duman, M. Acet, X. Moya, L. Mañosa, A. Planes, J. Appl. Phys. **102**, 033903 (2007)
6. M. Khan, N. Ali, S. Stadler, J. Appl. Phys. **101**, 053919 (2007)
7. W. Ito, Y. Imano, R. Kainuma, Y. Sutou, K. Oikawa, K. Ishida, Metall. Mater. Trans. A **38-A**, 760 (2007)
8. J. Liu, N. Scheerbaum, D. Hinz, O. Gutfleisch, Appl. Phys. Lett. **92**, 162509 (2008)
9. W. Ito, M. Nagasako, R.Y. Umetsu, R. Kainuma, T. Kanomata, K. Ishida, Appl. Phys. Lett. **93**, 232503 (2008)
10. A.K. Nayak, A.K. Nigum, K.G. Suresh, J. Phys. D Appl. Phys. **42**, 035009 (2009)
11. R. Kainuma, Y. Imano, W. Ito, H. Morito, Y. Sutou, K. Oikawa, A. Fujita, K. Ishida, S. Okamoto, O. Kitakami, Appl. Phys. Lett. **88–19**, 192513 (2006)
12. M. Mayer, *SIMNRA User's Guide, Report IPP 9/113* (Max-Planck-Institut Fur Plasmaphysik, Garching, Germany, 1997)

13. V. Garlea, B. Chakoumakos, S. Moore, G. Taylor, T. Chae, R. Maples, R. Riedel, G. Lynn, D. L. Selby, Appl. Phys. A **99**, 531 (2010)
14. Advanced Photon Source: http://www.aps.anl.gov/Beamlines/Directory/. (2004)
15. A.C. Larson, R.B. Von Dreele, General structure analysis system (GSAS), Los Alamos National Laboratory Report LAUR 86 (2004)
16. B.H. Toby, J. Appl. Cryst. **34**, 210 (2001)
17. J. Bai, J.M. Raulot, Y. Zhang, C. Esling, X. Zhao, L. Zuo, Appl. Phys. Lett. **98**, 164103 (2011)
18. S. Kaufmann, U. Rößler, O. Heczko, M. Wuttig, J. Buschbeck, L. Schultz, S. Fähler, Phys. Rev. Lett. **104**, 145702 (2010)
19. L. Righi, F. Albertini, S. Fabbrici, A. Paoluzi, Mater. Sci. Forum **684**, 105 (2011)
20. L. Righi, F. Albertini, E. Villa, A. Paoluzi, G. Calestani, V. Chernenko, S. Besseghini, C. Ritter, F. Passaretti, Acta Mater. **56**, 4529 (2008)
21. A. Kamantsev, V. Koledov, E. Dilmieva, A. Mashirov, V. Shavrov, J. Cwik, I. Tereshina, V. Khovaylo, M. Lyange, L. Gonzalez-Legarreta, B. Hernando, P. Ari-Gur, EPJ Web of Conferences **75**, 04008 (2014)